

PatchUp: A Regularization Technique for Convolutional Neural Networks

Mojtaba Faramarzi^{1,2}, Mohammad Amini^{1,3}, Akilesh Badrinaaraayanan^{1,2}, Vikas Verma^{1,2,4}

Sarath Chandar^{1,5,6}

¹Mila - Quebec AI Institute, ²University of Montreal, ³McGill University, ⁴Aalto University, Finland,
⁵École Polytechnique de Montréal, ⁶Canada CIFAR AI Chair

Abstract

Large capacity deep learning models are often prone to a high generalization gap when trained with a limited amount of labeled training data. A recent class of methods to address this problem uses various ways to construct a new training sample by mixing a pair (or more) of training samples. We propose *PatchUp*, a hidden state block-level regularization technique for Convolutional Neural Networks (CNNs), that is applied on selected contiguous blocks of feature maps from a random pair of samples. Our approach improves the robustness of CNN models against the *manifold intrusion* problem that may occur in other state-of-the-art mixing approaches like *Mixup* and *CutMix*. Moreover, since we are mixing the contiguous block of features in the hidden space, which has more dimensions than the input space, we obtain more diverse samples for training towards different dimensions. Our experiments on CIFAR-10, CIFAR-100, and SVHN datasets with PreactResnet18, PreactResnet34, and WideResnet-28-10 models show that *PatchUp* improves upon, or equals, the performance of current state-of-the-art regularizers for CNNs. We also show that *PatchUp* can provide better generalization to affine transformations of samples and is more robust against adversarial attacks.

1 Introduction

Deep Learning (DL), particularly deep Convolutional Neural Networks (CNNs) have achieved exceptional performance in many machine learning tasks, including object recognition [1], image classification [1–3], speech recognition [4] and natural language understanding [5, 6]. However, in a very deep and wide network, the network has a tendency to memorize the samples, which yields poor generalization for data outside of the training data distribution [7, 8]. To address this issue, noisy computation is often employed during the training, making the model more robust against invariant samples and thus improving the generalization of the model [9]. This idea is exploited in several state-of-the-art regularization techniques.

Such noisy computation based regularization techniques can be categorized into data-dependent and data-independent techniques [10]. Earlier work in this area has been more focused on the data-independent techniques such as Dropout [11], SpatialDropout [12], and DropBlock [13]. Dropout performs well on fully connected layers [14]. However, it is less effective on convolutional layers [15]. One of the reasons for the lack of success of dropout on CNN layers is perhaps that the activation units in the convolutional layers are correlated, thus despite dropping some of the activation units, information can still flow through these layers. SpatialDropout [15] addresses this issue by dropping the entire feature map from a convolutional layer. DropBlock [13] further improves SpatialDropout by dropping random continuous feature blocks from feature maps instead of dropping the entire feature map in the convolutional layers.

Recent works show that data-dependent regularizers can achieve better generalization for CNN models. Mixup [16], one such data-dependent regularizer, synthesizes additional training examples by interpolating random pairs of inputs x_i, x_j and their corresponding labels y_i, y_j as:

$$\tilde{x} = \lambda x_i + (1 - \lambda)x_j \quad \text{and} \quad \tilde{y} = \lambda y_i + (1 - \lambda)y_j \quad (1)$$

where $\lambda \in [0, 1]$ is sampled from a Beta distribution such that $\lambda \sim \text{Beta}(\alpha, \alpha)$ and (\tilde{x}, \tilde{y}) is the new example. By using these types of synthetic samples, Mixup encourages the model to behave linearly in-between the training samples.

The mixing coefficient λ in Mixup is sampled from a prior distribution. This may lead to the *manifold intrusion problem* [10]: the mixed synthetic example may *collide* (i.e. have the same value in the input space) with other examples in the training data, essentially leading to two training samples which have the same inputs but different targets. To overcome the manifold intrusion problem, Mai et al. [17] used a meta-learning approach to learn λ with a lower possibility of causing such collisions. However, this meta-learning approach adds significant computation complexity. ManifoldMixup [18] attempts to avoid the manifold intrusion problem by interpolating the hidden states (instead of input states) of a randomly chosen layer at every training update.

Different from the interpolation based regularizers discussed above, cutout [19] drops the contiguous regions from the image in the input space. This kind of noise encourages the network to learn the full context of the images instead of overfitting to the small set of visual features. CutMix [20] is another data-dependent regularization technique that cuts and fills rectangular shape parts from two randomly selected pairs in a mini-batch instead of interpolating two selected pairs completely. Applying CutMix at the input space improves the generalization of the CNN model by spreading the focus of the model across all places in the input instead of just a small region or a small set of intermediate activations. CutMix also improves the generalization performance of a very deep and wide CNN model such as PyramidNet. According to the CutMix paper, applying CutMix at the latent space, Feature CutMix, is not as effective as applying CutMix in the input space [20].

In this work, we propose *PatchUp* which is a regularization technique that operates in the hidden space by masking out contiguous blocks of the feature map of a random pair of samples, and then either mixes (*Soft PatchUp*) or swaps (*Hard PatchUp*) these selected contiguous blocks. Our experiments verify that *Hard PatchUp* achieves a better generalization performance compared to other state-of-the-art regularization techniques for CNNs such as Mixup, cutout, CutMix and ManifoldMixup on CIFAR-10, CIFAR-100, and SVHN datasets. *Soft PatchUp* achieves the second-best performance on CIFAR-10, CIFAR-100 with PreactResnet18, PreactResnet34, and WideResnet-28-10 models while achieving comparable results to ManifoldMixup on SVHN with PreactResnet18 and PreactResnet34. Furthermore, *PatchUp* provides significant improvements in the generalization on deformed images and better robustness against Fast Gradient Sign Method (FGSM) adversarial attack.

2 PatchUp

PatchUp is a hidden state block-level regularization technique that can be used after any convolutional layer in CNN models. Given a deep neural network $f(x)$ where x is the input, let g_k be the k -th convolutional layer. The network $f(x)$ can be represented as $f(x) = f_k(g_k(x))$ where g_k is the mapping from the input data to the hidden representation at layer k and f_k is the mapping from the hidden representation at layer k to the output [18]. In every training step, *PatchUp* applies block-level regularization at a randomly selected convolutional layer k from a set of intermediate convolutional layers. Appendix-B gives a formal intuition for selecting k randomly.

2.1 Binary Mask Creation

Once a convolutional layer k is chosen, the next step is to create a binary mask M (of the same size as the feature map in layer k) that will be used to *PatchUp* a pair of examples in the space of $g_k(x)$. The mask creation process is similar to that of DropBlock [13]. The idea is to select contiguous blocks of features from the feature map that will be either mixed or swapped with the same features in another example. To do so, we first select a set of features that can be altered (mixed or swapped). This is done by using the hyper-parameter γ which decides the probability of altering a feature. When we alter a feature, we also alter a square block of features centered around that feature which is controlled by the side length of this square block, *block_size*. Hence, the altering probabilities are

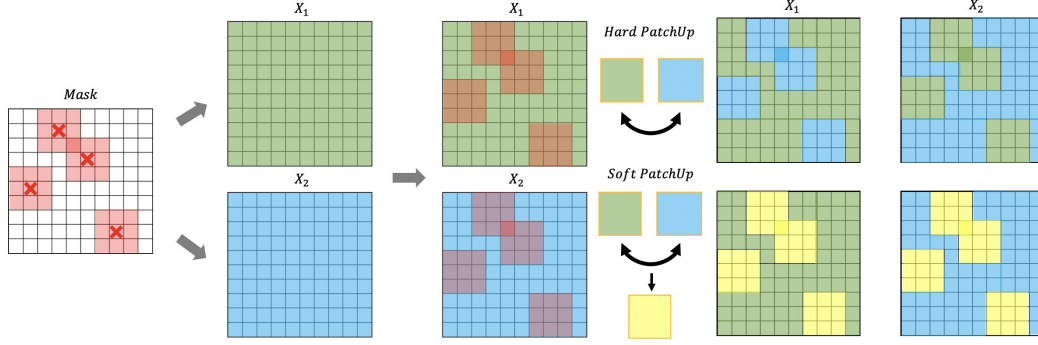


Figure 1: *PatchUp* process for two hidden representations associated with two samples randomly selected in the mini-batch (a, b). $X_1 = g_k^{(i)}(a)$ and $X_2 = g_k^{(i)}(b)$ where i is the feature map index. Right top shows *Hard PatchUp* output and the right bottom shows the interpolated samples with *Soft PatchUp*. The yellow continuous blocks represent the interpolated selected blocks.

readjusted using the following formula [13]:

$$\gamma_{adj} = \frac{\gamma \times (\text{feature map's area})}{(\text{block's area}) \times (\text{valid region to build block})}. \quad (2)$$

where the area of the feature map and block are the $feat_size^2$ and $block_size^2$, respectively, and the valid region to build the block is $(feat_size - block_size + 1)^2$.

For each feature in the feature map, we sample from $Bernoulli(\gamma_{adj})$. If the result of this sampling for feature f_{ij} is 0, then $M_{ij} = 1$. If the result of this sampling for f_{ij} is 1, then the entire square region in the mask with the center M_{ij} and the width and height of the square of $block_size$ is set to 0. Note that these feature blocks to be altered can overlap which will result in more complex block structures than just squares. The block structures created are called patches. Figure-1 illustrates an example mask used by *PatchUp*. The mask M has 1 for features outside the patches (which are not altered) and 0 for features inside the patches (which are altered).

2.2 PatchUp Operation

Once the mask is created, we can use the mask to select patches from the feature maps and either swap these patches (*Hard PatchUp*) or mix them (*Soft PatchUp*).

Consider two samples x_i and x_j . The *Hard PatchUp* operation at layer k is defined as follows:

$$\phi_{\text{hard}}(g_k(x_i), g_k(x_j)) = \mathbf{M} \odot g_k(x_i) + (\mathbf{1} - \mathbf{M}) \odot g_k(x_j), \quad (3)$$

where \odot is known as the element-wise multiplication operation and \mathbf{M} is the binary mask described in section 2.1.

To define *Soft PatchUp* operation, we first define the mixing operation for any two vectors a and b as follows:

$$\text{Mix}_\lambda(a, b) = \lambda \cdot a + (1 - \lambda) \cdot b, \quad (4)$$

where $\lambda \in [0, 1]$ is the mixing coefficient. Thus, the *Soft PatchUp* operation at layer k is defined as follows:

$$\phi_{\text{soft}}(g_k(x_i), g_k(x_j)) = \mathbf{M} \odot g_k(x_i) + \text{Mix}_\lambda[(\mathbf{1} - \mathbf{M}) \odot g_k(x_i), ((\mathbf{1} - \mathbf{M}) \odot g_k(x_j))]. \quad (5)$$

where λ in the range of $[0, 1]$ is sampled from a Beta distribution such that $\lambda \sim \text{Beta}(\alpha, \alpha)$. α controls the shape of the Beta distribution. Consequently, it controls the strength of interpolation [16]. Both *PatchUp* operations are illustrated in Figure 1.

2.3 Learning Objective

After applying the *PatchUp* operation, the CNN model continues the forward pass from layer k to the last layer in the model. The output of the model is used for the learning objective, including the loss minimization process and updating the model parameters accordingly.

Again, consider the example pairs (x_i, y_i) and (x_j, y_j) . Let $\phi_k = \phi(g_k(x_i), g_k(x_j))$ be the output of *PatchUp* after the k -th layer. Mathematically, the CNN with *PatchUp* minimizes the following loss function:

$$L(f) = \mathbb{E}_{(x_i, y_i) \sim P} \mathbb{E}_{(x_j, y_j) \sim P} \mathbb{E}_{\lambda \sim \text{Beta}(\alpha, \alpha)} \mathbb{E}_{k \sim S} \text{Mix}_{p_u}[\ell(f_k(\phi_k), y_i), \ell(f_k(\phi_k), Y)] + \ell(f_k(\phi_k), W(y_i, y_j)). \quad (6)$$

where p_u is the fraction of the unchanged features from feature maps in $g_k(x_i)$ and S is the set of layers where *PatchUp* is applied randomly. ϕ is ϕ_{hard} for *Hard PatchUp* and ϕ_{soft} for *Soft PatchUp*.

Y is the target corresponding to the changed features. In the case of *Hard PatchUp*, $Y = y_j$ and in the case of *Soft PatchUp*, $Y = \text{Mix}_\lambda(y_i, y_j)$. $W(y_i, y_j)$ calculates the re-weighted target according to the interpolation policy for y_i and y_j . W for *Hard PatchUp* and *Soft PatchUp* is defined as follows:

$$W_{\text{hard}}(y_i, y_j) = \text{Mix}_{p_u}(y_i, y_j). \quad (7)$$

$$W_{\text{soft}}(y_i, y_j) = \text{Mix}_{p_u}(y_i, \text{Mix}_\lambda(y_i, y_j)). \quad (8)$$

The *PatchUp* loss function has two terms where the first term is inspired from the CutMix loss function and the second term is inspired from the MixUp loss function.

2.4 PatchUp in Input Space

When $k = 0$, *PatchUp* only gets applied to the input space. To apply *PatchUp* to the input space, only the *Hard PatchUp* operation is used since swapping in the input space provides better generalization compared to mixing [20]. Only one random rectangular patch is selected in the input space (similar to CutMix) because the *PatchUp* binary mask is too strong for the input space, which has only three channels, compared to hidden layers in which each layer has numerous channels.

3 Relation to Other Methods

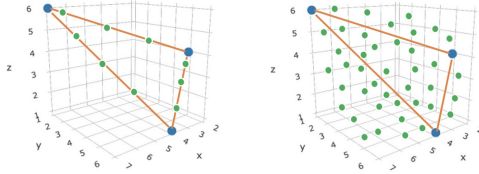


Figure 2: Left: ManifoldMixup interpolated samples for any combination of the three blue hidden states selected only from along orange line. Right: *PatchUp* can produce interpolated hidden representations for these three hidden states in almost all possible places in all dimensions except the samples which lie directly on the orange lines.



Figure 3: The two possible block selections from CutMix for two samples (cat and dog) with a large background. Swapping a similar part of the background or an essential element correlated to the label in the selected images can have a negative effect on the CutMix learning objective.

PatchUp Vs. ManifoldMixup: Both *PatchUp* and ManifoldMixup try to improve the generalization of a model by combining the latent representations of a pair of examples. ManifoldMixup combines two hidden representations by using the mixing operation defined in Equation 4 which produces a new latent representation in a linear way for a pair of two hidden representations. *PatchUp* uses a more complex approach to find a combination of two hidden representations, ensuring that a more diverse subspace of the hidden space gets explored. To understand the behaviour and the limitation that exist in the ManifoldMixup, assume that we have a 3D hidden space representation as illustrated in figure 2. Figure 2 presents the possible combinations of hidden representations explored via ManifoldMixup and *PatchUp*. Blue dots represent real hidden representation samples. ManifoldMixup can produce new samples that lie directly on the orange lines which connect the blue point pairs due to its linear interpolation strategy. On the other hand, *PatchUp* can select various points in all dimensions, and can also select points extremely close to the orange lines. The proximity to the orange lines depends on the selected pairs and λ sampled from the beta distribution. Appendix-C provides the mathematical and experimental justifications to show the comparative advantage of *PatchUp* over ManifoldMixup.

PatchUp Vs. CutMix: The CutMix strategy is to cut and fill some parts of the selected pairs instead of using interpolation for creating a new sample in the input space. Therefore, the CutMix method has less potential for a manifold intrusion problem, however, CutMix may still suffer from a manifold intrusion problem. Figure 3 shows two samples with small portions that correspond to their labels. CutMix cuts and fills the rectangular parts of the selected image randomly. In this example, if only the parts within the yellow bounding boxes are swapped, then the label does not change. However, if the parts within the white bounding boxes are swapped, then the entire label is swapped. In both scenarios, CutMix only learns the interpolated target based on the fraction of the images that is swapped. In contrast, these scenarios cannot occur in *PatchUp* since it works in the hidden representation space. Another difference between CutMix and *PatchUp* is how the masks are created. *PatchUp* can create arbitrarily shaped masks while CutMix masks can only be rectangular. Figure A.6 shows an example of CutMix Mask and *PatchUp* mask in input space and hidden representation space, respectively.

Feature-CutMix applies CutMix in the latent space. According to Yun et al. [20], Feature-CutMix is not as effective as CutMix. Both the learning objective of *PatchUp*, as well as the binary mask selection are different from Feature-CutMix.

4 Experiments

To evaluate the generalization improvements that *PatchUp* can provide with either *Hard* or *Soft PatchUp*, we applied *PatchUp* to image classification tasks on CIFAR-10, CIFAR-100 [21], and SVHN [22] datasets with PreActResNet18, PreActResNet34, and WideResNet-28-10 models¹. We used the same set of base hyper-parameters for all the models to be able to compare and evaluate the generalization improvements due to different regularization methods in a fair way. Appendix-D explains the experiment setup and the hyper-parameter tuning processes in detail. *PatchUp* adds *patchup_prob*, γ and *block_size* to the set of hyper-parameters. *patchup_prob* is the probability that *PatchUp* is performed for a given mini-batch. We set α to 2 in *PatchUp*. And, based on the hyper-parameter tuning described in Appendix-D, *Hard PatchUp* yields the best performance with *patchup_prob*, γ , and *block_size* as 0.7, 0.5, and 7, respectively. *Soft PatchUp* achieves the best performance with *patchup_prob*, γ , and *block_size* as 1.0, 0.75, and 7, respectively.

4.1 Generalization on Image Classification

Table 1 shows the comparison of the generalization performance of *PatchUp* with five other state-of-the-art regularization techniques on the CIFAR-10 and CIFAR-100 datasets. Our experiments show that *Hard PatchUp* leads to a lower test error for all the models on both CIFAR-10 and CIFAR-100. *Soft PatchUp* has the second-best result for this task. From Table 1, we see that *PatchUp* provides a significant improvement over previous state-of-the-art regularization techniques across different architectures. We observed that *Soft PatchUp* has the second-best performance across all the architectures indicating the potential that *Soft PatchUp* is beneficial in fine-grained classification. Table 2 shows that *Hard PatchUp* achieves the best top-1 error across the different models. Our experiments show that ManifoldMixup has the second-best performance for PreActResNet18 on SVHN. *Soft PatchUp* also achieves the second-best performance for WideResNet-28-10 on SVHN. It is also worth noting that *Soft PatchUp* performs reasonably well and is comparable to ManifoldMixup for PreActResNet34 on SVHN.

4.2 Generalization on Deformed Images

Regularization methods aim to improve the generalization of a model to unseen data. Applying affine transformations on the test set can provide novel deformed data that can be used to evaluate and compare the minimality and sufficiency of the representations learned by models with state-of-the-art regularization techniques [18]. We trained PreActResNet34 and WideResNet-28-10 on the CIFAR100 dataset. And then, we created deformed test sets from CIFAR100 by applying random rotations, random shearings, and different rescalings. Table 3 shows that *PatchUp* provides the best performance on affine transformed test sets and better generalization in PreActResNet34. Table 6 in Appendix-E illustrates that the quality of representations is improved by *PatchUp* and it also shows

¹The code to reproduce all the results is available at <https://github.com/chandar-lab/PatchUp>.

Table 1: Image classification task error rates on CIFAR-10 and CIFAR-100. We run experiments five times to report the mean and the standard deviation of errors and neg-log-likelihoods. Best performance result is shown in bold, second best is underlined. The lower number is better.

PreActResNet18	Test Error (%)	Test NLL	PreActResNet18	Test Error (%)	Test NLL
No Mixup	4.800 \pm 0.135	0.184 \pm 0.004	No Mixup	24.622 \pm 0.358	1.062 \pm 0.017
Input Mixup ($\alpha = 1$)	3.628 \pm 0.201	0.192 \pm 0.012	Input Mixup ($\alpha = 1$)	22.326 \pm 0.323	1.011 \pm 0.012
ManifoldMixup ($\alpha = 1.5$)	3.388 \pm 0.048	0.147 \pm 0.016	ManifoldMixup ($\alpha = 1.5$)	21.396 \pm 0.384	0.931 \pm 0.008
Cutout	4.218 \pm 0.046	0.158 \pm 0.005	Cutout	23.386 \pm 0.185	1.004 \pm 0.004
DropBlock	5.038 \pm 0.147	0.185 \pm 0.005	DropBlock	25.022 \pm 0.259	1.067 \pm 0.016
CutMix	3.518 \pm 0.898	0.131 \pm 0.002	CutMix	22.184 \pm 0.176	0.949 \pm 0.012
<i>Soft PatchUp</i>	<u>2.956 \pm 0.119</u>	0.169 \pm 0.031	<i>Soft PatchUp</i>	<u>19.950 \pm 0.180</u>	0.833 \pm 0.005
<i>Hard PatchUp</i>	2.918 \pm 0.131	0.146 \pm 0.718	<i>Hard PatchUp</i>	19.120 \pm 0.172	0.748 \pm 0.013
PreActResNet34			PreActResNet34		
No Mixup	4.640 \pm 0.099	0.204 \pm 0.004	No Mixup	23.342 \pm 0.269	1.103 \pm 0.006
Input Mixup ($\alpha = 1$)	3.260 \pm 0.075	0.175 \pm 0.004	Input Mixup ($\alpha = 1$)	21.000 \pm 0.440	0.950 \pm 0.019
ManifoldMixup ($\alpha = 1.5$)	2.926 \pm 0.062	0.124 \pm 0.004	ManifoldMixup ($\alpha = 1.5$)	18.724 \pm 0.305	0.810 \pm 0.008
Cutout	3.690 \pm 0.141	0.150 \pm 0.012	Cutout	22.420 \pm 0.075	1.043 \pm 0.001
DropBlock	4.950 \pm 0.188	0.221 \pm 0.010	DropBlock	23.744 \pm 0.125	1.113 \pm 0.007
CutMix	3.332 \pm 0.071	0.142 \pm 0.004	CutMix	19.944 \pm 0.141	0.907 \pm 0.008
<i>Soft PatchUp</i>	<u>2.570 \pm 0.062</u>	0.108 \pm 0.005	<i>Soft PatchUp</i>	<u>18.630 \pm 0.153</u>	0.816 \pm 0.016
<i>Hard PatchUp</i>	2.534 \pm 0.048	0.108 \pm 0.005	<i>Hard PatchUp</i>	17.692 \pm 0.125	0.758 \pm 0.016
WideResNet-28-10			WideResNet-28-10		
No Mixup	4.244 \pm 0.142	0.162 \pm 0.011	No Mixup	22.442 \pm 0.226	1.065 \pm 0.010
Input Mixup ($\alpha = 1$)	3.272 \pm 0.353	0.191 \pm 0.018	Input Mixup ($\alpha = 1$)	18.726 \pm 0.149	0.854 \pm 0.013
ManifoldMixup ($\alpha = 1.5$)	3.252 \pm 0.183	0.155 \pm 0.034	ManifoldMixup ($\alpha = 1.5$)	18.352 \pm 0.378	0.833 \pm 0.023
Cutout	3.134 \pm 0.119	0.122 \pm 0.005	Cutout	20.164 \pm 0.351	0.931 \pm 0.016
DropBlock	4.182 \pm 0.069	0.157 \pm 0.003	DropBlock	22.364 \pm 0.149	1.049 \pm 0.013
CutMix	3.148 \pm 0.118	0.126 \pm 0.004	CutMix	18.316 \pm 0.185	0.839 \pm 0.020
<i>Soft PatchUp</i>	<u>2.606 \pm 0.052</u>	0.132 \pm 0.029	<i>Soft PatchUp</i>	<u>16.726 \pm 0.110</u>	0.722 \pm 0.017
<i>Hard PatchUp</i>	2.528 \pm 0.095	0.114 \pm 0.014	<i>Hard PatchUp</i>	16.134 \pm 0.197	0.660 \pm 0.017

Comparison on CIFAR-10

Comparison on CIFAR-100

Table 2: Error rates comparison on SVHN. We run experiments five times to report the mean and the standard deviation of errors and neg-log-likelihoods. Best performance result is shown in bold, second best is underlined. The lower number is better.

	PreActResNet18		PreActResNet34		WideResNet-28-10	
	Error	Loss	Error	Loss	Error	Loss
No Mixup	3.035 \pm 0.092	0.138 \pm 0.004	3.087 \pm 0.659	0.164 \pm 0.008	2.833 \pm 0.081	0.137 \pm 0.008
Input Mixup ($\alpha = 1$)	2.930 \pm 0.221	0.233 \pm 0.016	2.855 \pm 0.096	0.223 \pm 0.024	2.643 \pm 0.161	0.207 \pm 0.041
ManifoldMixup ($\alpha = 2$)	2.436 \pm 0.056	0.157 \pm 0.062	2.423 \pm 0.428	0.146 \pm 0.064	2.425 \pm 0.101	0.157 \pm 0.029
Cutout	2.794 \pm 0.121	0.122 \pm 0.010	2.654 \pm 0.152	0.114 \pm 0.007	2.475 \pm 0.148	0.109 \pm 0.009
DropBlock	2.961 \pm 0.111	0.134 \pm 0.005	3.101 \pm 0.083	0.158 \pm 0.006	2.732 \pm 0.055	0.132 \pm 0.002
CutMix	3.040 \pm 0.054	0.135 \pm 0.031	2.658 \pm 0.049	0.121 \pm 0.005	2.433 \pm 0.045	0.110 \pm 0.003
<i>Soft PatchUp</i>	2.551 \pm 0.056	0.129 \pm 0.023	2.467 \pm 0.081	0.111 \pm 0.005	2.081 \pm 0.066	0.111 \pm 0.010
<i>Hard PatchUp</i>	2.286 \pm 0.084	0.107 \pm 0.004	2.123 \pm 0.024	0.101 \pm 0.007	<u>2.088 \pm 0.061</u>	0.105 \pm 0.012

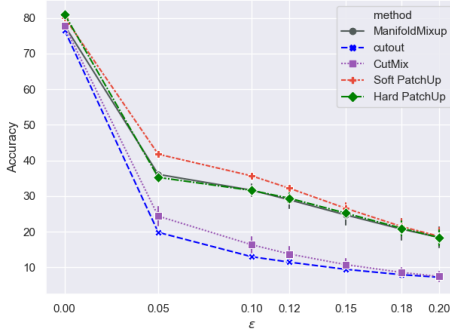
better generalization in deformed test sets on WideResNet-28-10. Generalization is significantly improved by *PatchUp*, as are the quality of representations learned by *PatchUp* as demonstrated by this experiment.

4.3 Robustness to Adversarial Examples

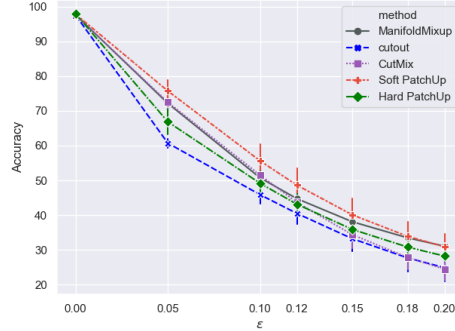
Since neural networks are trained based on Empirical Risk Minimization (ERM), slight changes in the data distribution have a significant effect on the model performance [23, 16]. Such unseen data used to confuse the models are known as adversarial examples. Certain data-dependent regularization techniques can alleviate such fragility to adversarial examples by training the models with interpolated data. Therefore, the robustness of a regularized model to adversarial examples can be considered as a criterion for comparison [16, 18, 20]. To evaluate the robustness of *PatchUp* against adversarial attacks, we compared the performance of PreActResNet18, PreActResNet34, and WideResNet-28-10 on CIFAR-10 and CIFAR-100 with adversarial examples created by the FGSM attack described in [24]. We compared the performance of WideResNet28-10 for SVHN against the FGSM attack. Figure 4 shows the robustness of *PatchUp* against FGSM attack. Figure A.11 in the appendix shows further comparisons. Based on the results, we can see that *Soft PatchUp* is more robust to adversarial attacks when compared to other regularization methods. *Hard PatchUp* and ManifoldMixup achieve

Table 3: Error rates in the test set on samples subject to affine transformations for PreActResNet34 trained on CIFAR-100 with indicated regularization method. We repeated each test for five trained models to report the mean and the standard deviation of errors. Best performance result is shown in bold, second best is underlined. The lower number is better.

Transformation	cutout	CutMix	ManifoldMixup	<i>Soft PatchUp</i>	<i>Hard PatchUp</i>
Rotate (-20, 20)	37.448 \pm 0.526	35.418 \pm 0.328	35.444 \pm 0.572	31.136 \pm 0.524	30.406 \pm 0.520
Rotate (-40, 40)	58.752 \pm 0.995	57.830 \pm 0.586	54.424 \pm 0.946	<u>53.422 \pm 0.420</u>	49.956 \pm 0.798
Shear (-28.6, 28.6)	36.552 \pm 0.487	34.148 \pm 0.473	34.150 \pm 0.416	28.984 \pm 0.497	29.574 \pm 0.410
Shear (-57.3, 57.3)	57.736 \pm 0.574	53.640 \pm 0.587	55.444 \pm 0.683	49.102 \pm 0.532	50.318 \pm 0.616
Scale (0.6)	72.994 \pm 1.231	54.304 \pm 1.268	78.998 \pm 1.126	46.246 \pm 1.204	50.062 \pm 2.692
Scale (0.8)	35.092 \pm 0.857	29.380 \pm 0.577	34.624 \pm 0.370	23.942 \pm 0.212	25.338 \pm 0.328
Scale (1.2)	42.310 \pm 0.706	49.522 \pm 2.035	<u>41.322 \pm 0.638</u>	43.414 \pm 0.652	38.002 \pm 0.703
Scale (1.4)	69.404 \pm 0.901	78.664 \pm 1.854	65.938 \pm 0.751	77.068 \pm 1.189	66.338 \pm 1.219



(a) Comparison on PreActResNet18 for CIFAR-100.



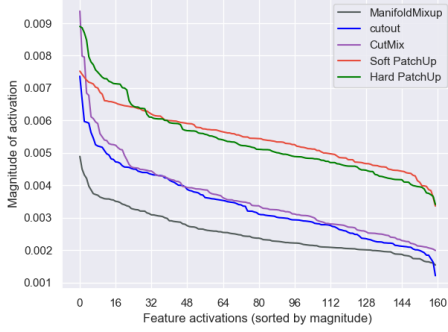
(b) Comparison on WideResNet28-10 for SVHN.

Figure 4: Robustness to FGSM attack. Plots are based on the mean and standard deviation of the accuracy of five trained models for each method against FGSM attack. The x-axis represents ϵ which is the magnitude that controls the perturbation.

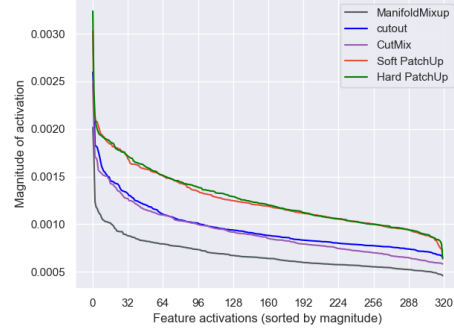
the second-best performance in most experiments. While *Hard PatchUp* achieves better performance in terms of classification accuracy, *Soft PatchUp* seems to trade-off a slight loss of accuracy in order to achieve more robustness.

4.4 Effect on Activations

To study the effect of the state-of-the-art regularization techniques on the activations in the residual blocks, we compared the mean magnitude of feature activations in the residual blocks following [19] in WideResNet28-10 for the test set in CIFAR-100. We first train the models with regularization techniques and then calculate the magnitudes of activations in the validation set. The higher mean magnitude of features shows that the models tried to produce a wider variety of features in the residual blocks [19]. Our WideResNet28-10 has a conv2d module followed by three residual blocks. For this ablation study, we selected k randomly such that $k \in \{0, 1, 2, 3\}$. Therefore, we apply the ManifoldMixup and *PatchUp* in either input space, first conv2d, first residual block, or second residual block. Figure 5 illustrates the comparison of ManifoldMixup, cutout, CutMix, *Soft PatchUp*, and *Hard PatchUp*. Figures 5a and 5b illustrate that *PatchUp* produces more diverse features in the layers where we apply *PatchUp*. In Appendix-G, figure A.12 shows this ablation study results in first conv2d, first residual block, second residual block and third residual block. Since we are not applying the *PatchUp* in the third residual block, the mean magnitude of the feature activations are below, but very close to, cutout and CutMix. This experiment also shows that producing a wide variety of features can be an advantage for a model. However, according to our experiments, a larger magnitude of activations does not always mean better performance. Figure 5 shows that for ManifoldMixup, the mean magnitude of the feature activations is less than other approaches. But, it performs better than cutout and CutMix in image classification, affine transformations, and FGSM attacks.



(a) Comparison on 1st Residual Block.



(b) Comparison on 2nd Residual Block.

Figure 5: The effect of the state-of-the-art regularization techniques on activations in WideResNet28-10 for CIFAR100 test set on the first and second Residual Blocks. Each curve is the magnitude of the feature activations, sorted in descending value, and averaged over all test samples for each method. The higher magnitude indicates a wider variety of the produced features by the model at each block.

4.5 Significance of loss terms

PatchUp uses the loss that is introduced in Equation 6. We can paraphrase the *PatchUp* learning objective for this ablation study as follow:

$$L(f) = \mathbb{E}_{(x_i, y_i) \sim P} \mathbb{E}_{(x_j, y_j) \sim P} \mathbb{E}_{\lambda \sim \text{Beta}(\alpha, \alpha)} \mathbb{E}_{k \sim \mathcal{S}} (L_1 + L_2), \quad (9)$$

where

$$L_1 = \text{Mix}_{p_u} [\ell(f_k(\phi_k), y_i), \ell(f_k(\phi_k), Y)], \quad (10)$$

$$L_2 = \ell(f_k(\phi_k), W(y_i, y_j)), \quad (11)$$

This section is an ablation study to show the effect of L_1 and L_2 in *PatchUp* loss. Table 4 shows the error rate on the validation set for WideResNet-28-10 on CIFAR-100. This study shows that the summation of the L_1 and L_2 reduces error rate by .1% in both *Soft PatchUp* and *Hard PatchUp*.

Table 4: The error rate on the validation set on CIFAR-100 for WideResNet-28-10 with *Hard PatchUp* and *Soft PatchUp*. The result is the mean and standard deviation of the experiment for five runs. A smaller number indicates better performance.

Simple WideResNet-28-10			Error Rate: 23.256 ± 0.586
	Error rates with L_1	Error rates with L_2	Error rates with $L(f)$
<i>Soft PatchUp</i>	16.856 ± 0.666	16.865 ± 0.339	16.75 ± 0.291
<i>Hard PatchUp</i>	16.135 ± 0.229	16.79 ± 0.457	16.02 ± 0.358

5 Conclusion

We presented *PatchUp*, a simple and efficient regularizer scheme for CNNs that alleviates some of the drawbacks of the previous mixing-based regularizers. Our experimental results show that with the proposed approach, *PatchUp*, we can achieve state-of-the-art results on image classification tasks across different architectures and datasets. Similar to previous mixing based approaches, our approach also has the advantage of avoiding any added computational overhead. The strong test accuracy achieved by *PatchUp*, with no additional computational overhead, makes it particularly appealing for practical applications.

Acknowledgments

We would like to acknowledge Compute Canada and Calcul Quebec for providing computing resources used in this work. The authors would also like to thank Damien Scieur, Hannah Alsdurf,

Alexia Jolicoeur-Martineau, and Yassine Yaakoubi for reviewing the manuscript. SC is supported by a Canada CIFAR AI Chair and an NSERC Discovery Grant.

References

- [1] Alex Krizhevsky, Ilya Sutskever, and Geoffrey E Hinton. Imagenet classification with deep convolutional neural networks. In F. Pereira, C. J. C. Burges, L. Bottou, and K. Q. Weinberger, editors, Advances in Neural Information Processing Systems 25, pages 1097–1105. Curran Associates, Inc., 2012.
- [2] Shaoqing Ren, Kaiming He, Ross Girshick, and Jian Sun. Faster r-cnn: Towards real-time object detection with region proposal networks. In C. Cortes, N. D. Lawrence, D. D. Lee, M. Sugiyama, and R. Garnett, editors, Advances in Neural Information Processing Systems 28, pages 91–99. Curran Associates, Inc., 2015.
- [3] Kaiming He, Xiangyu Zhang, Shaoqing Ren, and Jian Sun. Deep residual learning for image recognition. CoRR, abs/1512.03385, 2015. URL <http://arxiv.org/abs/1512.03385>.
- [4] G. Hinton, L. Deng, D. Yu, G. E. Dahl, A. Mohamed, N. Jaitly, A. Senior, V. Vanhoucke, P. Nguyen, T. N. Sainath, and B. Kingsbury. Deep neural networks for acoustic modeling in speech recognition: The shared views of four research groups. IEEE Signal Processing Magazine, 29(6):82–97, Nov 2012. ISSN 1558-0792. doi: 10.1109/MSP.2012.2205597.
- [5] Ilya Sutskever, Oriol Vinyals, and Quoc V. Le. Sequence to sequence learning with neural networks. In Proceedings of the 27th International Conference on Neural Information Processing Systems - Volume 2, NIPS’14, page 3104–3112, Cambridge, MA, USA, 2014. MIT Press.
- [6] Ashish Vaswani, Noam Shazeer, Niki Parmar, Jakob Uszkoreit, Llion Jones, Aidan N. Gomez, Lukasz Kaiser, and Illia Polosukhin. Attention is all you need. CoRR, abs/1706.03762, 2017. URL <http://arxiv.org/abs/1706.03762>.
- [7] Devansh Arpit, Stanisław Jastrzebski, Nicolas Ballas, David Krueger, Emmanuel Bengio, Maxinder S Kanwal, Tegan Maharaj, Asja Fischer, Aaron Courville, Yoshua Bengio, et al. A closer look at memorization in deep networks. In Proceedings of the 34th International Conference on Machine Learning-Volume 70, pages 233–242. JMLR. org, 2017.
- [8] Ian Goodfellow, Yoshua Bengio, and Aaron Courville. Deep learning. MIT press, 2016.
- [9] A. Achille and S. Soatto. Information dropout: Learning optimal representations through noisy computation. IEEE Transactions on Pattern Analysis and Machine Intelligence, 40(12): 2897–2905, Dec 2018. ISSN 1939-3539. doi: 10.1109/TPAMI.2017.2784440.
- [10] Hongyu Guo, Yongyi Mao, and Richong Zhang. Mixup as locally linear out-of-manifold regularization. CoRR, abs/1809.02499, 2018. URL <http://arxiv.org/abs/1809.02499>.
- [11] Nitish Srivastava, Geoffrey Hinton, Alex Krizhevsky, Ilya Sutskever, and Ruslan Salakhutdinov. Dropout: A simple way to prevent neural networks from overfitting. Journal of Machine Learning Research, 15:1929–1958, 06 2014.
- [12] Jonathan Tompson, Ross Goroshin, Arjun Jain, Yann LeCun, and Christoph Bregler. Efficient object localization using convolutional networks. CoRR, abs/1411.4280, 2014. URL <http://arxiv.org/abs/1411.4280>.
- [13] Golnaz Ghiasi, Tsung-Yi Lin, and Quoc V. Le. Dropblock: A regularization method for convolutional networks. CoRR, abs/1810.12890, 2018. URL <http://arxiv.org/abs/1810.12890>.
- [14] Nitish Srivastava, Geoffrey Hinton, Alex Krizhevsky, Ilya Sutskever, and Ruslan Salakhutdinov. Dropout: A simple way to prevent neural networks from overfitting. Journal of Machine Learning Research, 15:1929–1958, 2014. URL <http://jmlr.org/papers/v15/srivastava14a.html>.

- [15] Jonathan Tompson, Ross Goroshin, Arjun Jain, Yann LeCun, and Christoph Bregler. Efficient object localization using convolutional networks. CoRR, abs/1411.4280, 2014. URL <http://arxiv.org/abs/1411.4280>.
- [16] Hongyi Zhang, Moustapha Cisse, Yann N. Dauphin, and David Lopez-Paz. mixup: Beyond empirical risk minimization, 2017.
- [17] Zhijun Mai, Guosheng Hu, Dexiong Chen, Fumin Shen, and Heng Tao Shen. Metamixup: Learning adaptive interpolation policy of mixup with meta-learning, 2019.
- [18] Vikas Verma, Alex Lamb, Christopher Beckham, Amir Najafi, Ioannis Mitliagkas, David Lopez-Paz, and Yoshua Bengio. Manifold mixup: Better representations by interpolating hidden states. In Kamalika Chaudhuri and Ruslan Salakhutdinov, editors, Proceedings of the 36th International Conference on Machine Learning, volume 97 of Proceedings of Machine Learning Research, pages 6438–6447, Long Beach, California, USA, 09–15 Jun 2019. PMLR. URL <http://proceedings.mlr.press/v97/verma19a.html>.
- [19] Terrance DeVries and Graham W. Taylor. Improved regularization of convolutional neural networks with cutout, 2017.
- [20] Sangdoo Yun, Dongyoon Han, Seong Joon Oh, Sanghyuk Chun, Junsuk Choe, and Youngjoon Yoo. Cutmix: Regularization strategy to train strong classifiers with localizable features, 2019.
- [21] Alex Krizhevsky. Learning multiple layers of features from tiny images. 2009.
- [22] Yuval Netzer, Tao Wang, Adam Coates, Alessandro Bissacco, Bo Wu, and Andrew Y. Ng. Reading digits in natural images with unsupervised feature learning. In NIPS Workshop on Deep Learning and Unsupervised Feature Learning 2011, 2011.
- [23] Christian Szegedy, Wojciech Zaremba, Ilya Sutskever, Joan Bruna, Dumitru Erhan, Ian Goodfellow, and Rob Fergus. Intriguing properties of neural networks. arXiv preprint arXiv:1312.6199, 2013.
- [24] Ian J. Goodfellow, Jonathon Shlens, and Christian Szegedy. Explaining and harnessing adversarial examples, 2014.
- [25] Naftali Tishby and Noga Zaslavsky. Deep learning and the information bottleneck principle. CoRR, abs/1503.02406, 2015. URL <http://arxiv.org/abs/1503.02406>.

Appendices

A Algorithm

In this appendix, we provide a detailed algorithm for implementing *PatchUp*. As with most regularization techniques, *PatchUp* also has two modes (either inference or training). It also needs the combining type (either *Soft PatchUp* or *Hard PatchUp*), γ , and *block_size*. This algorithm shows how *PatchUp* generates a new hidden representation from $(g_k(x_i), y_i)$ and $(g_k(x_j), y_j)$. Lines 4 to 9 in the algorithm1 are the binary mask creation process used in both *Soft PatchUp* and *Hard PatchUp*.

Algorithm 1 *PatchUp*

Input:

$(g_k(x_i), y_i)$: the hidden representation for the sample (x_i, y_i) at layer k .
 $(g_k(x_j), y_j)$: the hidden representation for the sample (x_j, y_j) at layer k .
mode: either *inference* or *training*.
mixing_type: *soft* or *hard*.
 γ : the probability of altering a feature.
block_size: the size of each block in the binary mask.

Output

y_i, y_j : original labels for samples i and j .
 H' : the new hidden representation computed by *PatchUp*.
 p_u : The portion of the feature maps that remained unchanged.
 Y : the target corresponding to the changed features.
 W : re-weighted target according to the interpolation policy.

```

1: if mode == Inference then
2:   return  $(g_k(x_i), y_i), (g_k(x_j), y_j)$ 
3: end if
4: kernel_size  $\leftarrow$  (block_size, block_size)
5: stride  $\leftarrow$  (1, 1)
6: padding  $\leftarrow$  ( $\frac{\text{block\_size}}{2}, \frac{\text{block\_size}}{2}$ )
7:  $\gamma_{adj}$   $\leftarrow$  adjust  $\gamma$  using (2)
8: holes  $\leftarrow$  max_pool2d(Bernoulli( $\gamma_{adj}$ ), kernel_size, stride, padding)
9: Mask  $\leftarrow$   $1 - \text{holes}$ 
10: unchanged  $\leftarrow$  Mask  $\odot$   $g_k(x_i)$ 
11:  $p_u$   $\leftarrow$  calculate the portion of changed features map.
12: Patchi  $\leftarrow$  holes  $\odot$   $g_k(x_i)$ 
13: Patchj  $\leftarrow$  holes  $\odot$   $g_k(x_j)$ 
14: if mixing_type == hard then
15:   Patchi  $\leftarrow$  Patchj
16:    $Y \leftarrow y_j$ 
17:    $W \leftarrow W_{hard}(y_i, y_j)$  using (8)
18: else if mixing_type == soft then
19:    $\lambda \sim \text{Beta}(\alpha, \alpha)$ 
20:    $Y \leftarrow \text{Mix}_\lambda(y_i, y_j)$ 
21:    $W \leftarrow W_{soft}(y_i, y_j)$  using (8)
22:   Patchi  $\leftarrow$   $\text{Mix}_\lambda(\text{Patch}_i, \text{Patch}_j)$ 
23: end if
24:  $H' \leftarrow \text{unchanged} + \text{Patch}_i$ 
25: return  $y_i, y_j, H', p_u, Y, W$ 

```

Figure A.7 briefly illustrates and summarizes the binary mask creation process in *PatchUp*. Lines 11 to 25 correspond to the interpolation and combination of hidden representations in the mini-batch in *PatchUp*. Figure A.6 compares the masks generated by *PatchUp* and CutMix.

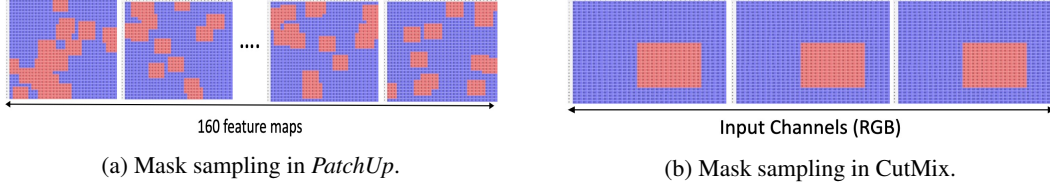


Figure A.6: Mask sampling in *PatchUp* is applied in the hidden state, compared to CutMix which is applied in the input space. Red areas show the blocks that should be altered.

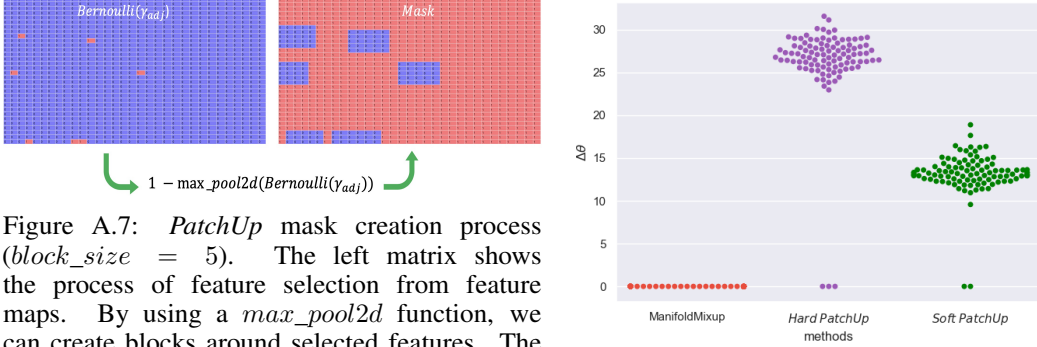


Figure A.7: *PatchUp* mask creation process ($block_size = 5$). The left matrix shows the process of feature selection from feature maps. By using a max_pool2d function, we can create blocks around selected features. The max_pool2d function uses $stride = (1, 1)$, $kernel_size = (block_size, block_size)$, and $padding = (\frac{block_size}{2}, \frac{block_size}{2})$. Red and blue points are 1 and 0 in the generated binary mask, respectively.

Figure A.8: The comparison of ρ for flattened hidden representations of a mini-batch of samples at the second residual block (layer $k = 3$) of WideResNet-28-10 with corresponding regularization method.

B Why random k ?

PatchUp applies block-level regularization at a randomly selected hidden representation layer k . The Information Bottleneck (IB) principle, introduced by Tishby and Zaslavsky [25], gives a formal intuition for selecting k randomly. First, let us encapsulate the layers of the network into blocks where each block could contain more than one layer. Let g_k be the k -th block of layers. In this case, sequential blocks share the information as a hidden representation to the next block of layers, sequentially. We can consider this case as a Markov chain of the block of layers as follows:

$$x \rightarrow g_1(x) \rightarrow g_2(x) \rightarrow g_3(x). \quad (12)$$

In this scenario, the sequential communication between the intermediate hidden representations are considered to be an information bottleneck. Therefore,

$$I(g_3(x); g_2(x)) < I(g_2(x); g_1(x)) < I(g_1(x); x), \quad (13)$$

where $I(g_k(x); g_{k-1}(x))$ is the mutual information between the k -th and $(k - 1)$ -th layer.

If $g_{k=3}(x)$ has enough information to represent x , then applying regularization techniques in $g_{k=3}(x)$ will provide a better generalization to unseen data. However, most of the current state-of-the-art CNN models contain residual connections which break the Markov chain described above (since information can skip the $g_{k=3}$ layer). One solution to this challenge is to randomly select a residual block and apply regularization techniques like ManifoldMixup or *PatchUp*.

C *PatchUp* Interpolation Policy Effect

Assume that \mathcal{H}_1 and \mathcal{H}_2 are flattened hidden representations of two examples produced at layer k . And, \mathcal{H} is the flattened interpolated hidden representation of these two paired samples at layer k . First, we calculate the cosine distance of the pairs $(\mathcal{H}_2, \mathcal{H}_1)$, $(\mathcal{H}_1, \mathcal{H})$, and $(\mathcal{H}_2, \mathcal{H})$. Reversing the cosine of these cosine similarities give the angular distance between each pair of vectors denoted as

$\angle\theta$, $\angle\alpha_1$, and $\angle\alpha_2$, respectively. There is always a surface that contains \mathcal{H}_2 and \mathcal{H}_1 denoted as \mathcal{S} . Mathematically, we have:

$$\angle\alpha_1 = \cos^{-1}\left(\frac{\mathcal{H}_1 \cdot \mathcal{H}}{\|\mathcal{H}_1\| \|\mathcal{H}\|}\right) \quad \& \quad \angle\alpha_2 = \cos^{-1}\left(\frac{\mathcal{H}_2 \cdot \mathcal{H}}{\|\mathcal{H}_2\| \|\mathcal{H}\|}\right) \quad \& \quad \angle\theta = \cos^{-1}\left(\frac{\mathcal{H}_2 \cdot \mathcal{H}_1}{\|\mathcal{H}_2\| \|\mathcal{H}_1\|}\right), \quad (14)$$

Let us define $\angle\rho = (\angle\alpha_1 + \angle\alpha_2) - \angle\theta$ and $\angle\rho' = |\angle\alpha_1 - \angle\alpha_2| - \angle\theta$. According to the triangle inequality principle, either $\angle\rho$ or $\angle\rho'$ will be zero if, and only if, $\mathcal{H} \in \mathcal{S}$. Figure A.9 illustrates three possible scenarios for two paired flattened hidden representations and their flattened interpolated hidden representations. $\angle\rho$ and $\angle\rho'$ are zero for the left and right figures, respectively. We try to empirically show that \mathcal{H}_2 , \mathcal{H}_1 , and \mathcal{H} always lie in the same surface \mathcal{S} and \mathcal{H} lies between \mathcal{H}_2 and \mathcal{H}_1 in ManifoldMixup. This means that $\angle\rho = 0$ for ManifoldMixup because of its linear interpolation policy. The middle figure in A.9 is the case that both $\angle\rho$ and $\angle\rho'$ are not equal to zero. This figure shows that one possible situation is that flattened interpolated hidden representation does not lie in the surface \mathcal{S} . Our goal is to produce the interpolated hidden representation that lies in all possible places towards all dimensions in the hidden space.

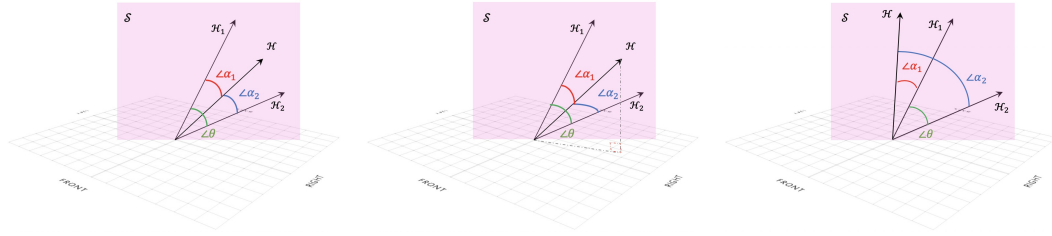


Figure A.9: \mathcal{H}_1 and \mathcal{H}_2 are the flattened hidden representations. \mathcal{H} is the flattened interpolated hidden representation that can be produced by either ManifoldMixup, *Soft PatchUp* or *Hard PatchUp*.

As discussed in section 3, ManifoldMixup can provide interpolated hidden representation only in a limited space. However, *Soft PatchUp* and *Hard PatchUp* can produce a wide variety of interpolated hidden representations towards different dimensions. To support that, in WideResNet-28-10, for a mini-batch of 100 samples, we calculated the $\angle\rho$ for the flattened interpolated hidden representation produced by ManifoldMixup, *Hard PatchUp*, and *Soft PatchUp* at the second residual block (layer $k = 3$) with the same interpolation policy ($\lambda = .4$, $\gamma = .5$, and $block_size = 7$) for both *Soft PatchUp* and *Hard PatchUp* for all samples in the mini-batch. The swarmplot A.8 shows all $\angle\rho$ for the mini-batch are equal to zero in ManifoldMixup, which empirically supports our hypothesis. However, *PatchUp* produces more diverse interpolated hidden representations towards all dimensions in the hidden space. It is worth mentioning that few $\angle\rho$ that are equal to zero in *Soft PatchUp* and *Hard PatchUp* belong to the interpolated hidden representation that was constructed from the pairs with the same labels.

D *PatchUp* Experiment Setup and Hyper-parameter Tuning

This section describes the hyper-parameters of each model in table 5 following the hyper-parameter setup from ManifoldMixup [18] experiments in order to create a fair comparison. First, we performed hyper-parameter tuning for the *PatchUp* to achieve the best validation performance. Then we ran all the experiments five times, reporting the mean and standard deviation of errors and negative log likelihoods for the selected models. We let models train for defined epochs and checkpoint the best model in terms of validation performance during the training. In our study, we used PreActResNet18, PreActResNet34, and WideResNet-28-10 models. Table 5 shows the hyper-parameters used for training the models.

PatchUp adds *patchup_prob*, γ and *block_size* as hyper-parameters. *patchup_prob* is the probability that the *PatchUp* operation is performed for a given mini-batch, i.e if there are N mini-batches and *patchup_prob* is p , *PatchUp* is performed in p fraction of N mini-batches. γ and *block_size* are described in section 2. We tuned the *PatchUp* hyper-parameter on CIFAR-10 with the PreActResNet18. To create a validation set, we split 10% of training samples into a validation set. We set α to 2 in *PatchUp*. For *Soft PatchUp*, we set *patchup_prob* to 1.0 and applied *PatchUp* to all mini-batches in training. Then, we did a grid search by varying γ from 0.45 to 0.9 and *block_size*

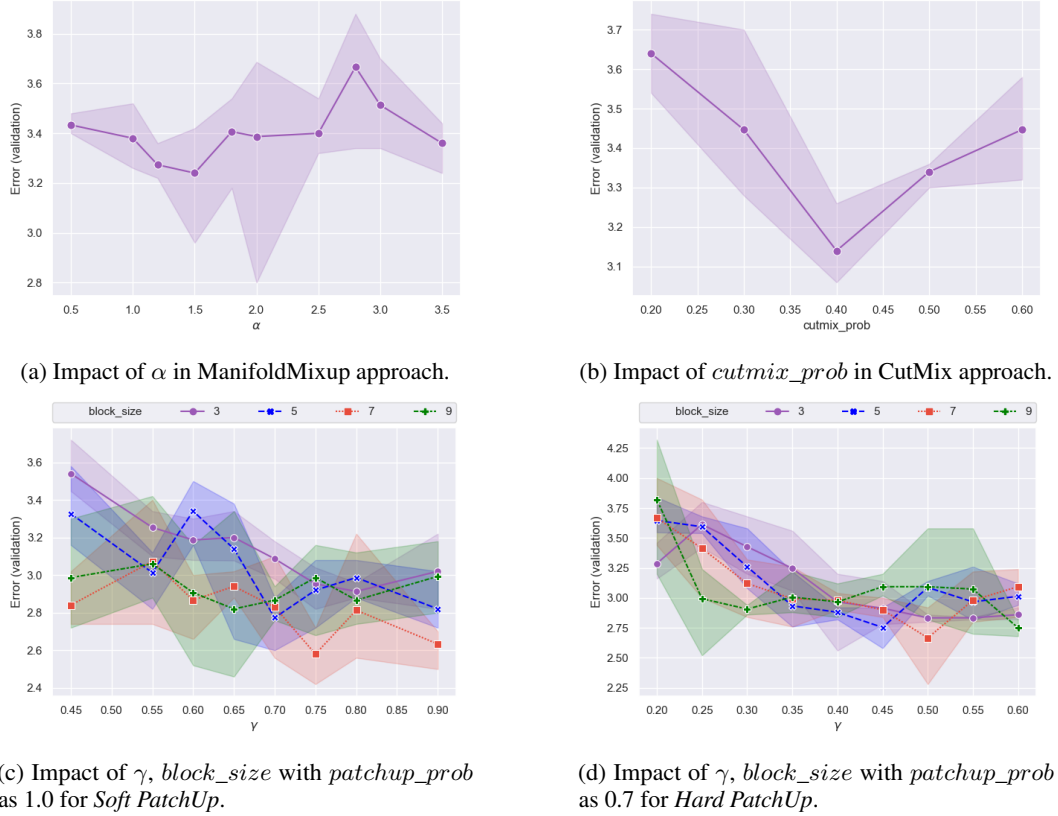


Figure A.10: Impact of hyper-parameters γ , $block_size$ and $patchup_prob$ on error rates in the CIFAR-10 validation set for PreActResNet18. We repeated each job three times to collect the mean and the standard deviation of errors. Marked points are the mean of the error rate in the validation set. And, the shadow shows the bootstrapping of results for each hyper-parameter setting. The lower numbers on the y-axes correspond to better performance.

Table 5: The hyper-parameters used for each model to compare the effect of each regularization technique. The learning rate is denoted as lr . And, lr is multiplied at each learning rate schedule step by the step factor.

Model	lr	lr steps	step factor	Epochs
PreactResnet18	0.1	500-1000-1500	0.1	2000
PreactResnet34	0.1	500-1000-1500	0.1	2000
WideResnet-28-10	0.1	200-300	0.1	400

from 3 to 9. We found that γ of 0.75 and $block_size$ of 7 work best for *Soft PatchUp* as shown in figure A.10c. Similarly, for *Hard PatchUp*, we set $patchup_prob$ to 0.7 and performed a grid search by varying γ from 0.2 to 0.6 and $block_size$ from 3 to 9. We found that $block_size$ of 7 and γ of 0.5 yield the best results for *Hard PatchUp* as shown in figure A.10d. Figure A.10a shows that ManifoldMixup with ($\alpha = 1.5$) achieves the best validation performance. For cutout, we used the same hyper-parameters proposed in [19], setting cutout to 16 for CIFAR10, 8 for CIFAR100, and 20 for SVHN following [19]. Figure A.10b shows that CutMix achieves its best validation performance in PreActResNet18 in CIFAR-10 with $cutmix_prob = 0.4$. Furthermore, DropBlock achieves its best validation performance on this task by setting the block size and γ to 7 and 0.9, respectively [13].

Table 6: Error rates in the test set on samples subject to affine transformations for WideResNet-28-10 trained on CIFAR-100 with indicated regularization method. We repeated each test for five trained models to report the mean and the standard deviation of errors. Best performance result is shown in bold, second best is underlined. The lower number is better.

Transformation	cutout	CutMix	ManifoldMixup	<i>Soft PatchUp</i>	<i>Hard PatchUp</i>
Rotate (-20, 20)	36.162 \pm 0.633	34.236 \pm 0.785	35.774 \pm 0.621	31.282 \pm 0.622	31.340 \pm 0.318
Rotate (-40, 40)	57.220 \pm 0.549	56.512 \pm 0.752	56.610 \pm 0.877	52.014 \pm 0.916	<u>53.804 \pm 0.576</u>
Shear (-28.6, 28.6)	33.482 \pm 0.463	31.770 \pm 0.312	32.300 \pm 0.317	<u>30.898 \pm 0.836</u>	28.426 \pm 0.430
Shear (-57.3, 57.3)	53.328 \pm 0.587	<u>50.618 \pm 0.552</u>	52.366 \pm 0.170	<u>51.908 \pm 0.632</u>	48.334 \pm 0.631
Scale (0.6)	56.770 \pm 0.376	45.980 \pm 0.404	63.924 \pm 2.160	52.648 \pm 0.616	<u>46.924 \pm 1.035</u>
Scale (0.8)	30.550 \pm 0.611	26.818 \pm 0.328	29.012 \pm 0.372	27.188 \pm 0.597	23.840 \pm 0.535
Scale (1.2)	47.268 \pm 0.639	51.258 \pm 0.817	41.644 \pm 0.846	<u>42.108 \pm 0.985</u>	43.370 \pm 1.223
Scale (1.4)	79.000 \pm 0.933	82.562 \pm 0.575	<u>72.752 \pm 0.846</u>	70.970 \pm 1.433	77.370 \pm 1.457

E Generalization on Deformed Images

We created the deformed test sets from CIFAR100, as described in Section 4.2. Table 6 shows improved quality of representations learned by a WideResNet-28-10 model regularized by *PatchUp* on CIFAR-100 deformed test sets. The significant improvements in generalization provided by *PatchUp* in this experiment shows the high quality of representations learned with *PatchUp*.

F Robustness to Adversarial Examples

The adversarial attacks refer to small and unrecognizable perturbations on the input images that can mislead deep learning models [24, 8]. One approach to creating adversarial examples is using the Fast Gradient Sign Method (FGSM), also known as a white-box attack [24]. FGSM creates examples by adding small perturbations to the original examples. Once a regularized model is trained then FGSM creates adversarial examples as follows [24]:

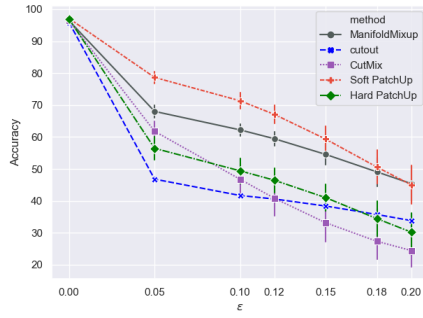
$$x' = x + \epsilon \times \text{sign}(\nabla_{\mathbf{x}} J(\boldsymbol{\theta}, \mathbf{x}, y)). \quad (15)$$

where x' is an adversarial example, x is the original example, y is the ground truth label for x , and $J(\boldsymbol{\theta}, \mathbf{x}, y)$ is the loss of the model with parameters of $\boldsymbol{\theta}$. ϵ controls the perturbation.

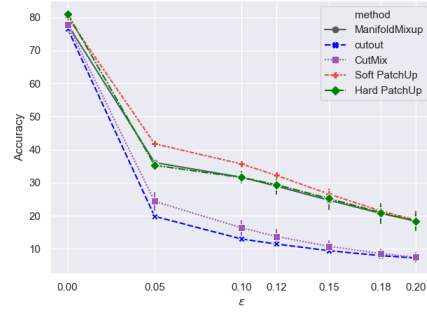
Our experiments show the effectiveness of *Soft PatchUp* against the attacks in most cases. However, *Hard PatchUp* performed well against the FGSM attack only on PreActResNet34 for CIFAR-100. Figure A.11 shows the comparison of the state-of-the-art regularization techniques' effect on model robustness against the FGSM attack.

G Analysis of *PatchUp*'s Effect on Activations

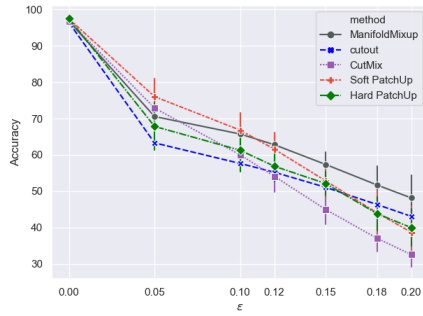
In our implementation WideResNet28-10 has a conv2d module followed by three residual blocks. Figure A.12 illustrates the comparison of ManifoldMixup, cutout, CutMix, *Soft PatchUp*, and *Hard PatchUp*. Figure A.12a, A.12b, and A.12c show that *PatchUp* produces more variety of features in layers that we apply *PatchUp* on.



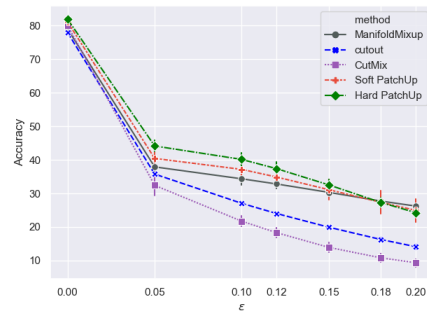
(a) Comparison on PreActResNet18 for CIFAR-10.



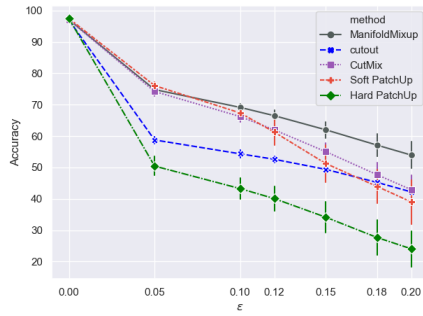
(b) Comparison on PreActResNet18 for CIFAR-100.



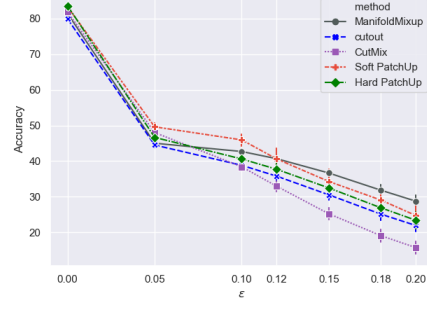
(c) Comparison on PreActResNet34 for CIFAR-10.



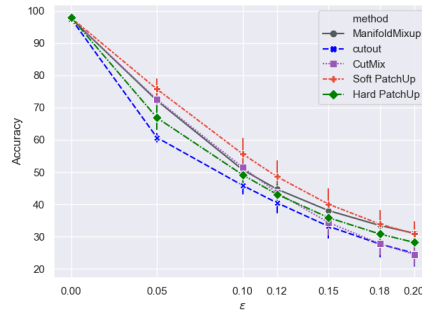
(d) Comparison on PreActResNet34 for CIFAR-100.



(e) Comparison on WideResNet28-10 for CIFAR-10.

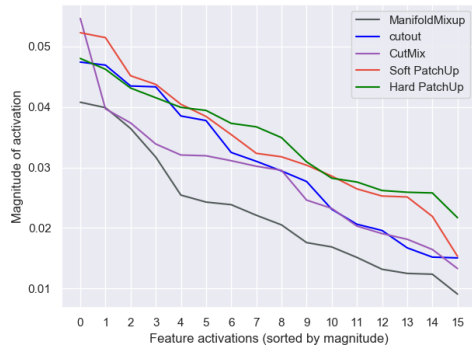


(f) Comparison on WideResNet28-10 for CIFAR-100.

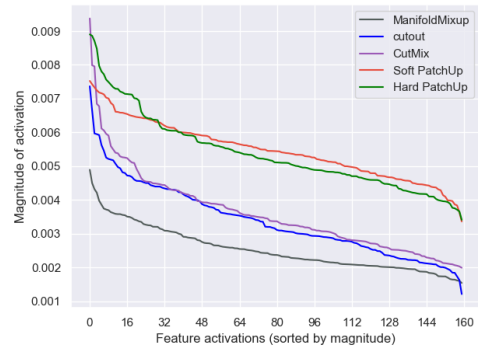


(g) Comparison on WideResNet28-10 for SVHN.

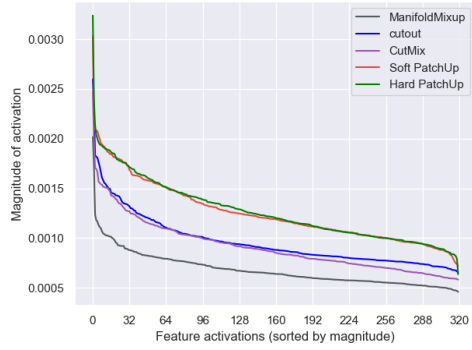
Figure A.11: Robustness to the FGSM attack, known as a white-box attack. We repeated each test for five trained models to report the mean and the standard deviation of the accuracy of each method against the FGSM attack. The higher values on the y-axes show the robustness of the model against the attack. And, ϵ is the magnitude that controls the perturbation.



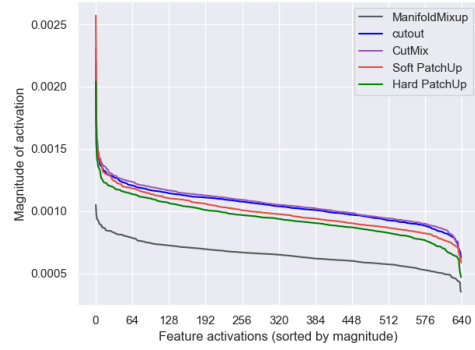
(a) Comparison on the first convolution module.



(b) Comparison on 1st Residual Block.



(c) Comparison on 2nd Residual Block.



(d) Comparison on 3rd Residual Block.

Figure A.12: The effect of the state-of-the-art regularization techniques on activations in WideResNet28-10 for CIFAR100 test set. Each curve is the magnitude of feature activations, sorted by descending value, and averaged over all test samples for each method. The higher magnitude shows a wider variety of the produced features by the model at each block.